

5 | Kiribati



5.1 Summary

5.1.1 Climate

- Kiribati has a hot, humid climate with relatively small changes in air temperature from season to season and strong links to changes in the surrounding ocean temperature. The seasonal cycle of rainfall is variable across the large region. The wettest months at Kiritimati are March and April and at Tarawa between December and April.
- The seasonal cycle of rainfall is affected by the Intertropical Convergence Zone (ITCZ), with the strongest impact at Tarawa.
- Annual and seasonal air temperatures at Tarawa increased over the period 1951–2019.
- Annual and seasonal rainfall trends, as well as trends in rainfall extremes, show little change at Tarawa and Kiritimati. There is a strong influence from the El Niño–Southern Oscillation (ENSO) on annual rainfall and the duration of dry spells at both sites.
- As the Kiribati Islands are located within a few degrees of the equator, tropical cyclones rarely form within or pass through Kiribati waters.

5.1.2 Ocean

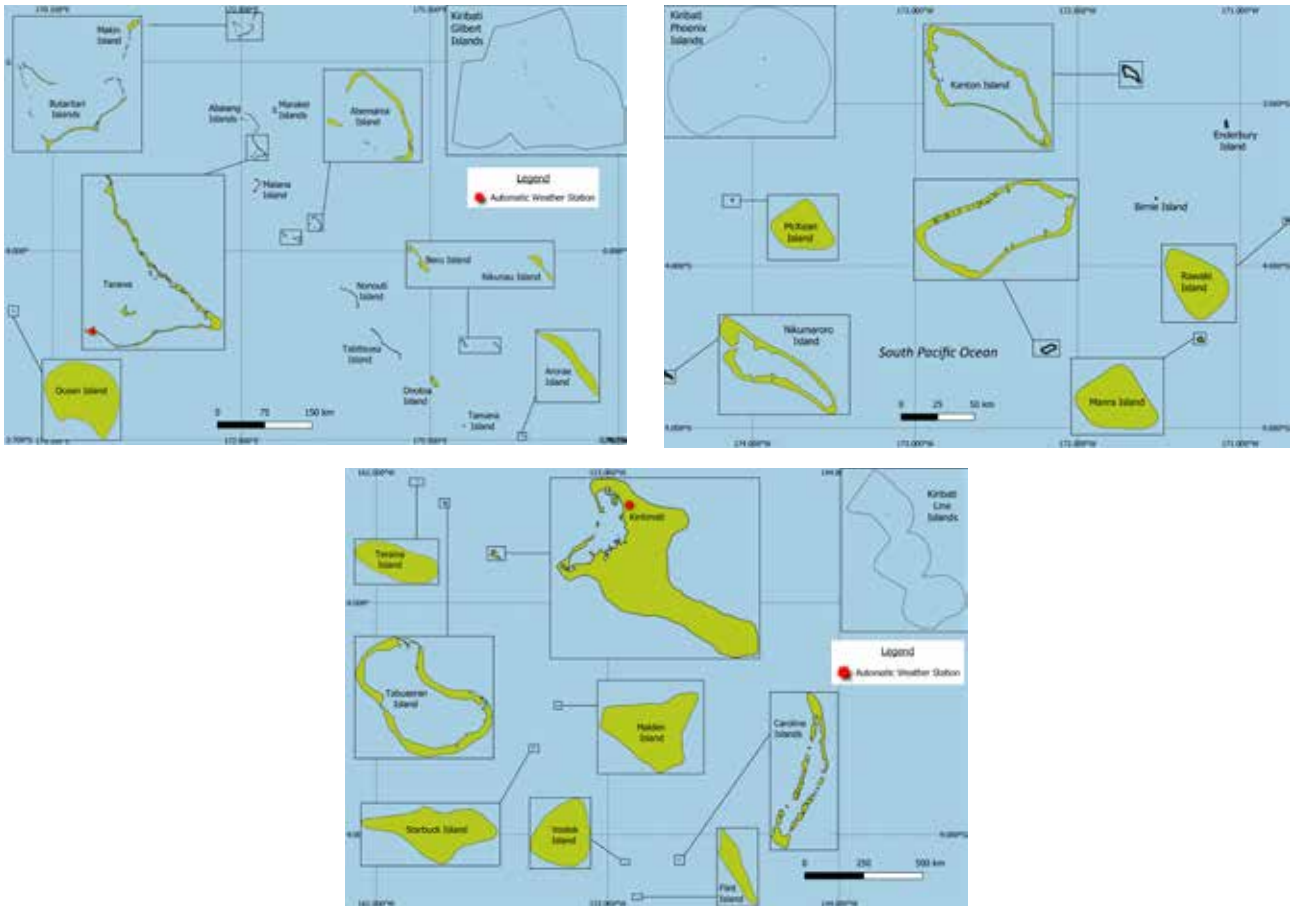
- Highest sea levels typically occur between January and March and in August/September. El Niño years typically have higher sea levels during February/March.
- Sea-level rise in the Kiribati exclusive economic zone (EEZ), as measured by satellite altimeters from 1993 to mid-2020, ranges from about 3 to 4 mm per year in the vicinity of the Gilbert and Phoenix Islands, and up to 4.5 mm per year in the vicinity of the Line Islands.
- Monthly average ocean temperature, as measured by the Tarawa tide-gauge, ranges from 29 °C in February to 30 °C in the months from June to October. Monthly ocean temperatures in any given year can be up to ± 2.5 °C of these averages.
- The sea surface temperature (SST) trend across the EEZ is 0.21 °C per decade.
- Dominant wave direction is from 209° (SSW), with an average significant wave height of 0.78 m and average wave period of 12.17 s.
- Severe wave height was defined as 1.41 m, with an average of 3.9 severe events per year.
- Peak average wave period occurs from January to June, with little seasonal change in the significant wave height.

5.2 Country description

The Republic of Kiribati is located in the equatorial Pacific Ocean, with islands north and south of the equator and both west and east of the 180th meridian (Figure 5.1). Kiribati comprises 32 atolls and one raised coral island between latitudes 5°N and 12°S, and longitudes 120°E and 150°W. The groups of islands include Banaba Island between Nauru and the Gilbert Islands (16 atolls), Phoenix Islands (8 atolls and coral islands) and the Line Islands

(8 atolls and a reef). Kiribati has a total land area of 811 km² and an EEZ of 3.4 million km². Tarawa, the largest atoll at 31 km², includes the capital, South Tarawa. The highest elevation is 81 m above sea level on Banaba. Kiribati's population is approximately 120,000. About 90% of the population live in the Gilbert Islands, with more than 50% in South Tarawa (Betio).

Figure 5.1: Kiribati Gilbert Islands (top left), Phoenix Islands (top right) and Line Islands (bottom center) and the locations of the climate stations used in this report



5.3 Data

Daily historical rainfall and air temperature records for Tarawa (Gilbert Islands) and Kiritimati (Line Islands) from 1951 were obtained from the Kiribati Meteorological Service. These records have undergone data quality and homogeneity assessment. Where the maximum or minimum air temperature records were found to have discontinuities, these records have been adjusted to make them homogeneous (further information is provided in Chapter 1). Additional information on historical climate trends for Kiribati can be found in the Pacific Climate Change Data Portal <http://www.bom.gov.au/climate/pccsp>.

Tropical cyclone data and historical tracks starting from the 1969/70 season are available from the SHTC Data Portal <http://www.bom.gov.au/cyclone/history/tracks/index.shtml>.

SST covering the EEZ was obtained via the daily Optimum Interpolation SST version 2.1 (OISST v2.1) dataset from NOAA (Reynolds et al. 2007; Banzon et al. 2016). In situ ocean

temperature data were obtained from the PSLGM Project tide-gauge located at Tarawa, with data spanning from 1993 to 2021.

Wave data were obtained from the PACCSAP wave hindcast (Smith et al. 2021), available hourly from 1979 to 2021, with a grid resolution near Kiribati of 7 km.

Regional sea level data were obtained from CSIRO satellite altimetry (updated by Benoit Legresy, Church and White 2011), with correction for seasonal signals, inverse barometer effect and glacial isostatic adjustment. Tide-gauge data were sourced from the Tarawa tide-gauge station, spanning from 1993 to 2020 at hourly intervals.

5.4 Rainfall

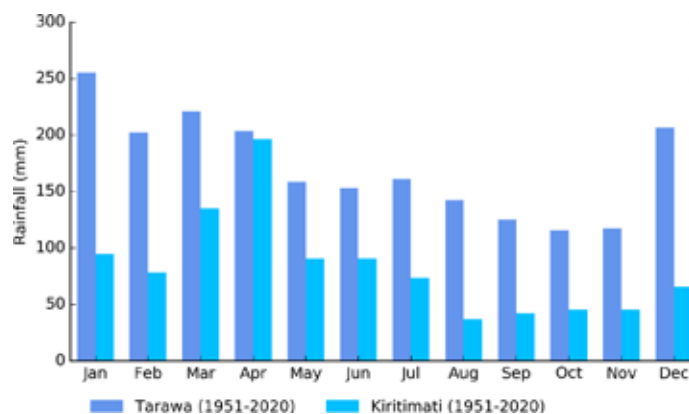
5.4.1 Seasonal cycle

The driest and wettest periods in the year vary from location to location. The driest six-month period at Tarawa is June–November, known locally as Aumaiaki, with the driest month of October averaging 115 mm. The wettest season, Aumeang, lasts from December to approximately May, with peak rainfall in January averaging 255 mm. Approximately 58% of

rainfall falls during the December to May period (Figure 5.2). The wettest months of the year occur when the ITCZ is furthest south and close to Tarawa.

At Kiritimati Island, the peak rainfall month is April, with the lowest rainfall months during the last five months of the year. Approximately 69% of rainfall occurs during the wettest season.

Figure 5.2: Mean annual rainfall at Tarawa and Kiritimati



5.4.2 Trends

Trends in annual and seasonal rainfall since 1951 are not statistically significant at Tarawa and Kiritimati (Figure 5.3, Table 5.1). Annual and seasonal rainfall trends indicate little

change. Strong variability associated with ENSO is evident at both sites, with El Niño years generally experiencing much higher rainfall than La Niña years. Annual rainfall varies from approximately 500 to 4400 mm at Tarawa and from approximately 200 to 3700 mm at Kiritimati.

Figure 5.3: Annual rainfall (bar graph) and number of wet days (where rainfall is at least 1 mm; line graph) at Tarawa (left) and Kiritimati (right). Straight lines indicate linear trends for annual rainfall (in black) and number of wet days (in blue). Criteria for statistical robustness were not met for determining a linear trend for number of wet days at Kiritimati. The magnitudes of the trends are presented in Table 5.1. Diamonds indicate years with insufficient data for one or both variables.

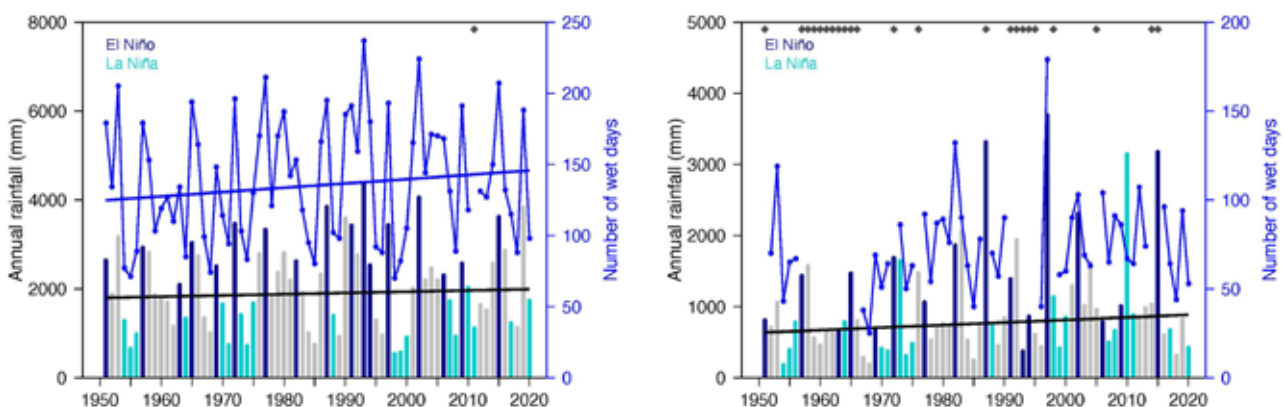


Table 5.1:

Trends in annual, seasonal and extreme rainfall at Tarawa (left) and Kiritimati (right). The 95% confidence intervals are shown in parentheses. The contribution to total rainfall from extreme events and the standardised rainfall evapotranspiration index are measured relative to 1961–1990 (see Chapter 1 for details). Criteria for statistical robustness were not met for determining linear trends for rainfall extremes at Kiritimati. The standardised rainfall evapotranspiration index is not available for Kiritimati due to the unavailability of daily temperature observations at this site.

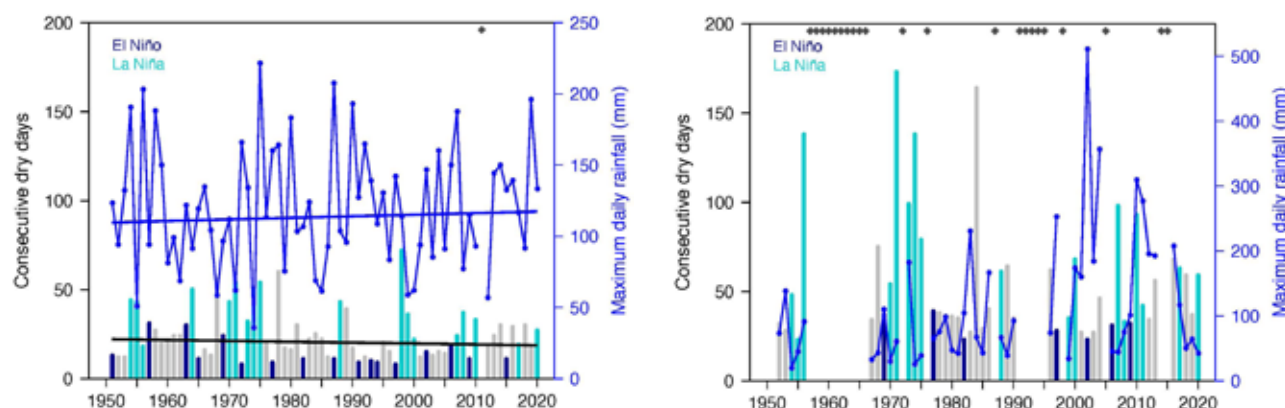
	Tarawa	Kiritimati
	1951–2020	
Annual rainfall (mm/decade)	+28.30 (-102.38, +160.96)	+35.82 (-12.65, +86.68)
November–April (mm/decade)	+2.46 (-92.75, +94.50)	+35.32 (-0.43, +70.60)
May–October (mm/decade)	+23.78 (-30.94, +76.87)	+3.00 (-18.00, +26.34)
Number of wet days (days/decade)	+3.03 (-2.44, +9.07)	-
Contribution to total rainfall from extreme events (%/decade)	-0.14 (-1.32, +1.08)	-
Consecutive dry days (days/decade)	-0.49 (-2.11, +0.75)	-
Maximum one-day rainfall (mm/decade)	+1.12 (-4.56, +6.56)	-
Standardised rainfall evapotranspiration index (November–April)	0.00 (-0.19, +0.19)	-
Standardised rainfall evapotranspiration index (May–October)	+0.07 (-0.06, +0.18)	-

Numerous gaps exist in the daily rainfall record for Kiritimati, which prevents the robust calculation of trends in rainfall extremes (Table 5.1). No significant trends in extreme rainfall were detected at Tarawa. Figure 5.4 shows change and variability in the longest run of days without rain and maximum

daily rainfall at Tarawa and Kiritimati. At both sites, variability associated with ENSO is evident, with La Niña years experiencing much longer dry spells than El Niño years. Year-to-year variability in consecutive dry days is higher at Kiritimati than Tarawa, with several years experiencing over four months without rain.

Figure 5.4:

Annual longest run of consecutive dry days (bar graph) and maximum daily rainfall (line graph) at Tarawa (left) and Kiritimati (right). Straight lines indicate linear trends for dry days (black) and maximum daily rainfall (blue). The magnitudes of the trends are presented in Table 5.1. Criteria for statistical robustness were not met for determining linear trends at Kiritimati. Diamonds indicate years with insufficient data for one or both variables.



5.5 Air temperature

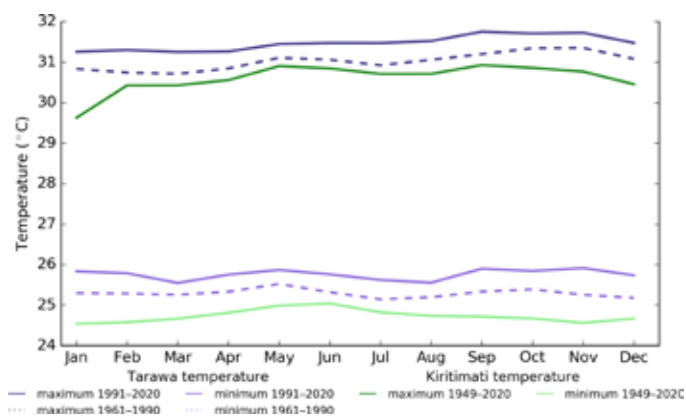
5.5.1 Seasonal cycle

Kiribati has a hot, humid tropical climate, with air temperatures very closely related to the temperature of the oceans surrounding the small islands and atolls. At both Tarawa and Kiritimati Island, average maximum and minimum air temperatures are highly stable throughout the year, with a range of less than 1 °C (Figure 5.5).

There has been a clear shift towards warmer average monthly temperatures between 1961–1990 and 1991–2020, with warmer average air temperatures occurring in all months throughout the year for Tarawa.

Figure 5.5:

Maximum and minimum air temperature seasonal cycle for Tarawa (purple) and Kiritimati (green), and for the periods 1961–1990 (dotted lines) and 1991–2020 (solid lines)



** High amount of missing temperature data for Kiritimati. The average 1949–2020 temperature cycle is available.

5.5.2 Trends

Average annual and seasonal temperatures have increased significantly at Tarawa (Figure 5.6, Table 5.2). The relatively small size of year-to-year fluctuations in temperature at Tarawa can be attributed to its equatorial location.

Figure 5.6:

Average annual, November–April and May–October temperatures for Tarawa. Straight lines indicate linear trends. The magnitudes of the trends are presented in Table 1.2. Diamonds indicate years with insufficient data for one or more variables.

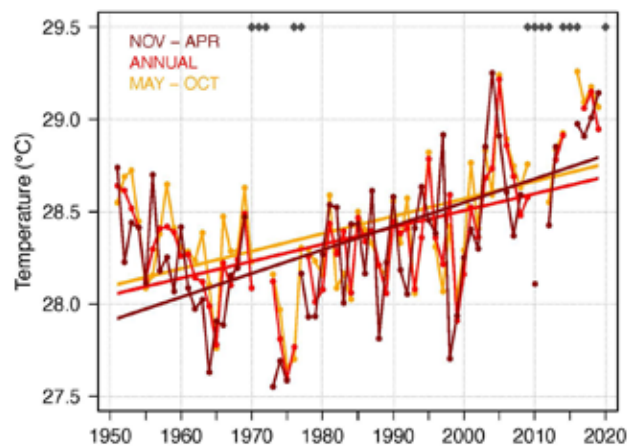


Table 5.2:

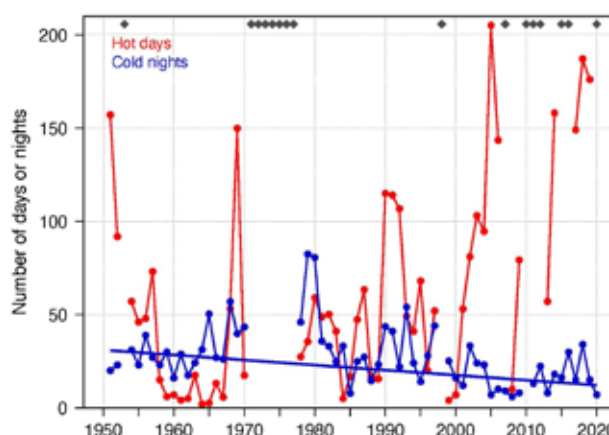
Trends in annual and seasonal air temperatures at Tarawa. The 95% confidence intervals are shown in parentheses, and trends significant at the 95% level are shown in bold.

	Tarawa Tmax (°C/decade)	Tarawa Tmin (°C/decade)	Tarawa Tmean (°C/decade)
1951–2019			
Annual	+0.12 (+0.02, +0.22)	+0.11 (+0.03, +0.19)	+0.09 (+0.01, +0.17)
November–April	+0.13 (+0.04, +0.21)	+0.11 (+0.05, +0.18)	+0.13 (+0.05, +0.20)
May–October	+0.11 (0.00, +0.21)	+0.10 (+0.02, +0.16)	+0.09 (+0.02, +0.17)

Numerous gaps exist in the daily temperature record at Tarawa, which prevents the robust calculation of trends for most temperature extremes. Nevertheless, Figure 5.7 shows that the number of cold nights has been decreasing, although this trend is not significant. The number of hot days varies substantially from year to year. This may be partly explained by the equatorial location of Tarawa, which requires only small temperature increases for a day to be considered hot, i.e., in the top 10% of days compared to 1961–1990 (see Chapter 1 for details).

Figure 5.7:

Annual number of hot days and cold nights at Tarawa. The straight line indicates the linear trend. Criteria for statistical robustness were not met for determining a linear trend for hot days. Diamonds indicate years with insufficient data for one or both variables.



5.6 Tropical cyclones

5.6.1 Seasonal cycle

Tropical cyclones affect Kiribati during the southern hemisphere tropical cyclone season, which is from November to April, but the occurrence of cyclones is rare due to the country’s geographic position near the equator. The tropical cyclone archive of the

southern hemisphere indicates that between the 1969/70 and 2017/18 seasons, five tropical cyclones passed within the EEZ, with occurrences recorded in El Niño years 1977/78, 1982/83, 1991/92 and 1997/98 (Line Group), and 1987/88 (Phoenix Group) seasons. In addition, two tropical cyclones located in the Northwest Pacific basin passed near Tarawa in 1979 and 2015.

5.6.2 Trends

Trends in total number of tropical cyclones (<995 hPa) and severe tropical cyclones (<970hPa) are presented for the period 1981/82–2020/21 for the greater Southwest Pacific (135°E–120°W; 0–50°S). Trends are presented at a regional scale as the number of tropical cyclones occurring within Pacific Island EEZs is insufficient for reliable long-term trend analysis.

For the total number of tropical cyclones, the trend (and 95% confidence interval) is -0.92 (-1.85, 0.01) tropical cyclones/decade. There has been little change/marginal decline in the total number of tropical cyclones over the last 40 seasons. This trend is not statistically significant.

For the total number of severe tropical cyclones, the trend is -0.80 (-1.32, -0.29) tropical cyclones/decade. There is a negative trend in the number of severe tropical cyclones over the last

40 seasons. There has been little change/marginal decline in the proportion of tropical cyclones reaching severe status. The trend is -0.04 (-0.08, 0.00) tropical cyclones/decade. The negative trend is statistically significant.

Records of tropical cyclones exist from the late 1800s in some countries in the Southwest Pacific, but trends in tropical cyclones have only been presented from 1981/82. Satellite-based observations began in the Southwest Pacific in the early 1970s, but consistent coverage and reliable intensity estimates have only been available since the early 1980s. Confidence in tropical cyclone trends is moderate as the definition of a tropical cyclone has changed and satellite observation methods have continued to improve over the last 40 years.

5.7 Sea surface temperature

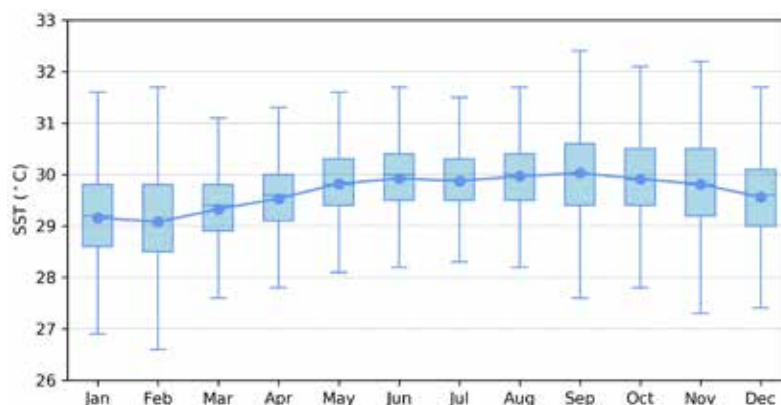
5.7.1 Seasonal cycle

Ocean temperature, as measured by the Tarawa tide-gauge, reaches on average a maximum of approximately 30 °C from June to October, but individual months can get as high as above 32 °C from September to November (Figure 5.8). Minimum average temperature is 29 °C in

February. Temperatures can be up to 2.5 °C higher or lower than these averages, although 50% of observations fall within 1.5 °C of the average. Equatorial locations typically have little average variation but can drastically change in a given year depending on the ENSO cycle. The variability in temperatures between September and February is reflective of the peak months of ENSO.

Figure 5.8:

Annual temperatures measured at the Tarawa tide-gauge. Blue dots show the monthly average, and shaded boxes show the middle 50% of observations. Lines show the top and bottom 25% of observations.

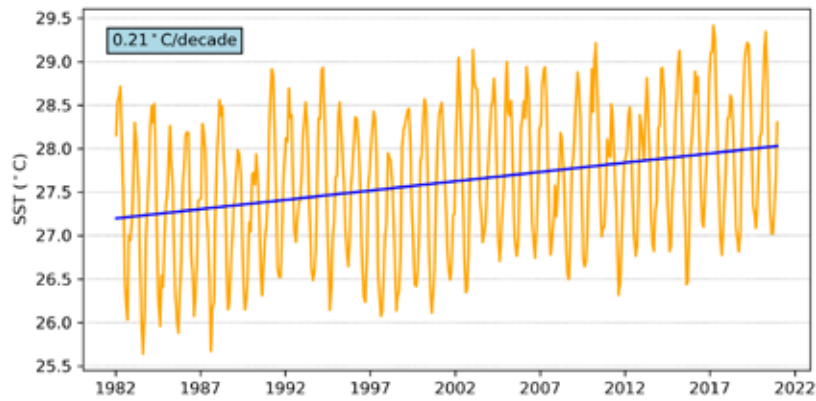


5.7.2 Trends

Figure 5.9 shows the 1981–2021 SST from satellite observations averaged over the EEZ regions. The data show a trend of 0.21 °C per decade with a 95% confidence interval of ± 0.06 °C.

Figure 5.9:

Sea surface temperature from satellite observations averaged across Kiribati EEZ, shown as the orange line. The blue line shows the linear regression trend.



5.8 Sea level

5.8.1 Seasonal cycle

Kiribati experiences a semidiurnal tidal cycle, meaning two high and two low tides per day. The highest predicted tides of the year at Tarawa typically occur in August/September as well as December–February. For Kiritimati, highest predicted tides are around August, and also from November to January. Figure 5.10 shows the number of hours the 99th percentile (2.93 m) sea level

threshold is exceeded per month across the entire sea level record at Tarawa. Peak sea levels typically occur from January to March but also in August/September. El Niño years typically have higher sea levels during February/March. Since approximately 2009, the number of hours that exceed the 99th percentile threshold has been increasing. This is due to a combination of sea-level rise and subsidence occurring at Kiribati (Brown et al. 2020).

Figure 5.10: Number of hours exceeding 99th percentile sea level threshold per month from 1993 to 2020 at the Tarawa tide-gauge. Blue shading indicates the number of hours, and the final row provides a percentage summary of all the years.

Number of hours exceeding 2.93 m (Betio, Kiribati)													
	Jan	Feb	Mar	Apr	May	Jun	Jul	Aug	Sep	Oct	Nov	Dec	Annual
1993	0	0	0	0	0	0	0	0	0	0	0	0	0
1994	0	0	0	0	0	0	0	0	0	0	0	3	3
1995	0	0	0	0	0	0	0	0	0	0	0	0	0
1996	1	0	0	0	0	0	0	0	0	0	0	0	1
1997	4	1	4	0	0	0	0	0	0	0	0	0	9
1998	0	0	0	0	0	0	0	0	0	0	0	0	0
1999	0	0	0	0	0	0	0	0	0	0	0	0	0
2000	0	0	0	0	0	0	0	0	0	0	0	0	0
2001	0	0	0	0	0	0	0	0	1	0	0	0	1
2002	0	0	0	0	0	0	0	1	2	0	0	0	3
2003	0	0	0	0	0	0	0	0	0	0	0	0	0
2004	0	0	0	0	0	0	0	0	0	0	0	0	0
2005	0	2	0	0	0	0	0	0	0	0	0	0	2
2006	0	2	2	0	0	0	0	0	2	1	1	0	8
2007	0	1	0	0	0	0	0	0	0	0	0	0	1
2008	0	0	0	0	0	0	0	0	0	0	0	0	0
2009	1	0	0	0	0	1	2	2	5	0	0	1	12
2010	3	2	2	0	0	0	0	0	0	0	0	0	7
2011	0	3	0	1	0	0	0	0	0	0	0	0	4
2012	0	0	0	1	0	0	0	0	0	0	0	0	1
2013	0	0	0	0	0	0	0	0	0	0	0	0	0
2014	0	6	6	0	0	0	1	3	1	0	0	0	17
2015	1	7	4	1	0	0	0	3	6	0	0	0	22
2016	0	0	0	0	0	0	0	0	0	0	0	0	0
2017	0	0	0	0	0	0	0	0	0	0	1	2	3
2018	2	0	0	0	0	0	0	1	2	0	0	0	5
2019	6	8	0	0	0	0	0	2	7	0	1	0	24
2020	0	4	1	0	0	0	0	0	0	0	2	0	7
Monthly Totals (%)	14	28	15	2	0	1	2	9	20	1	4	5	

5.8.2 Trends

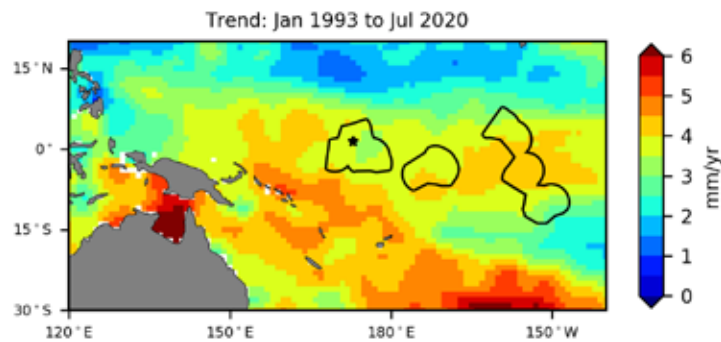
Sea level across the three Kiribati island groups, measured by satellite altimeters (Figure 5.11) since 1993, has risen between 3 and 4 mm per year in the Gilbert and Phoenix Islands and far north/south of the Line Islands. Trends are between 4 and 4.5 mm per year in central Line Islands and far southern Phoenix Islands. This is larger than the global average of 3.1 ± 0.4 mm per year (von Schuckmann et al. 2021). The 95% confidence interval is between 0.6 and 1.0 mm for the Gilbert and Phoenix Islands, and up to 1.2 mm for central Line Islands. This rise is partly linked

to a pattern related to climate variability from year to year and decade to decade.

Trend estimates at the Tarawa tide-gauge over a similar time span to the altimetry observations (December 1992 to July 2020) are provided in the PSLGM Monthly Data Report for July 2020 (<http://www.bom.gov.au/ntc/IDO60101/IDO60101.202007.pdf>). For Tarawa, the trend is reported as 4.4 mm per year, slightly higher than the altimetry trends shown in Figure 5.11 (tide-gauge indicated by star symbol). This difference is most likely attributed to subsidence occurring at Tarawa (Brown et al. 2020).

Figure 5.11:

Satellite altimetry annual trend for the Pacific from 1993 to 2020, with Kiribati EEZ highlighted. The star symbol indicates the location of the tide-gauge at Tarawa.



5.9 Waves

5.9.1 Seasonal cycle

The average wave climate at Betio is defined by the significant wave height, peak period and peak direction. The significant wave height is the mean wave height (from trough to crest) of the highest one third of waves and corresponds to the wave height that would be reported by an experienced observer. Peak period is the time interval between two waves of the dominant wave period. Peak direction is the direction from which the dominant waves are coming.

The average sea state is dominated by swells from the south. The annual mean wave height is 0.78 m, the annual mean wave direction is 209° and the annual mean wave period is 12.17 s. In the Pacific, waves often come from multiple directions and for different periods of time. In Betio, there are often more than seven different wave direction/period components with the majority coming from between south to southeast (Figure 5.12).

The significant wave height shows little change between the seasons at Betio. However, wave period is significantly higher from March to June (Figure 5.13). Wave height peaks in winter, and wave period peaks in May.

Figure 5.12: Annual wave rose for Betio. Note that direction is where the wave is coming from.

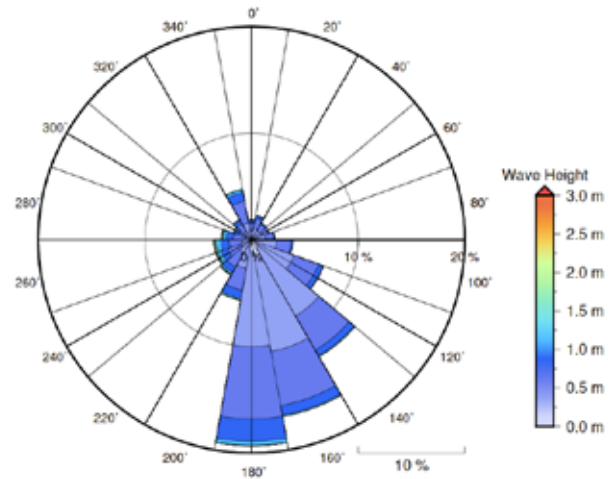
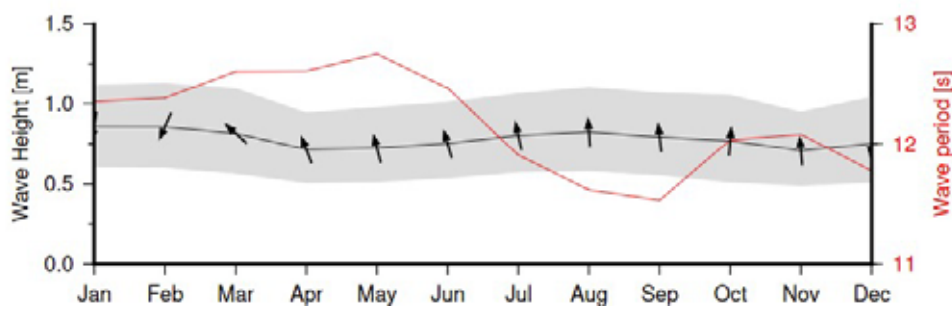


Figure 5.13: Monthly wave height (black line), wave period (red line) and wave direction (arrows). The grey area represents the range of wave height between calm periods (10% of lowest wave height) and large wave events (10% of highest wave height).



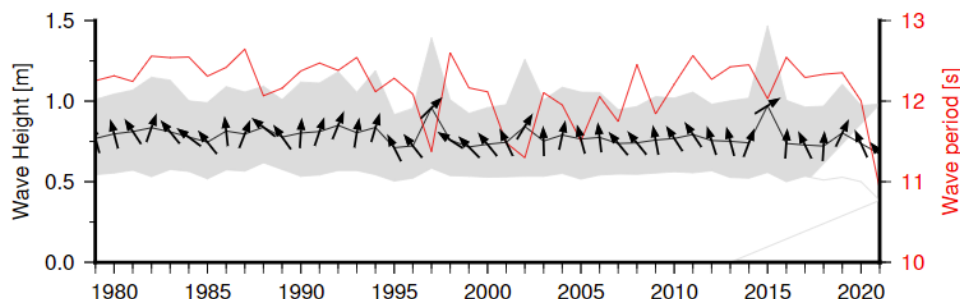
5.9.2 Trends

Waves change from month to month with the seasons and also from year to year with climate oscillations. Typically, these changes are smaller than the seasonal changes but can be

important during phenomena such as ENSO. At Betio, the mean annual wave height has remained unchanged since 1979 (Figure 5.14). The mean annual wave height in Betio is not significantly correlated with the main climate indicators of the region.

Figure 5.14:

Annual wave height (black line), wave period (red line) and wave direction (arrows). The grey area represents the range of wave height between calm periods (10% of lowest wave height) and large wave events (10% of highest wave height).



5.9.3 Extreme waves

Extreme wave analysis for Betio was done by defining a severe height threshold and fitting a generalized Pareto distribution (GPD). The optimum threshold selected was 1.41 m. In the 42-year wave hindcast, 163 wave events reached or exceeded this threshold, averaging 3.9 per year. The GPD was fitted to the largest wave height reached

during each of these events (Figure 5.15, Table 5.14). Extreme wave analysis is a very useful tool but is not always accurate because the analysis is very sensitive to the data available, the type of distribution fitted and the threshold used. For example, this analysis does not accurately account for tropical cyclone waves. More in-depth analysis is required to obtain results appropriate for designing coastal infrastructure and coastal hazard planning.

Figure 5.15:

Extreme wave distribution for Betio. The crosses represent the wave events that have occurred since 1979. The solid line is the statistical distribution that best fits past wave events. The dashed lines show the upper and lower confidence limits of the fit. There is a 95% chance that the fitted distribution lies between the two dashed lines. Note that the annual return interval is in logarithmic scale.

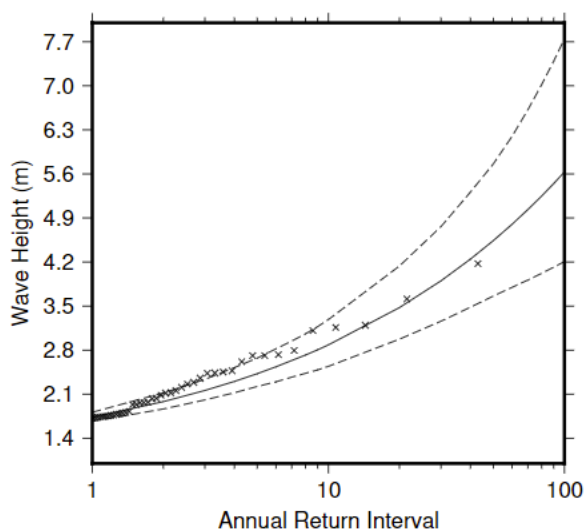


Table 5.3:

Summary of the results from extreme wave analysis in Betio

Large wave height (90 th percentile)	1.26 m
Severe wave height (99 th percentile)	1.74m
1-year ARI wave height	2.24 m
10-year ARI wave height	3.75 m
20-year ARI wave height	4.66 m
50-year ARI wave height	6.46 m
100-year ARI wave height	8.48 m